Solid Polymer Electrolytes Hot Paper

DOI: 10.1002/ange.201307423

Transferring Lithium Ions in Nanochannels: A PEO/Li^+ Solid Polymer Electrolyte Design**

Ling-Yun Yang, Da-Xiu Wei, Min Xu, Ye-Feng Yao, and Qun Chen**

Abstract: *A new category of crystalline polymer electrolyte prepared by the supramolecular self-assembly of polyethylene oxide (PEO), α-cyclodextrin (α-CD), and $LiAsF_6$ is reported. The polymer electrolyte consists of the nanochannels formed by α-CDs in which the PEO/Li^+ complexes are confined. The nanochannels formed by α-CD provide the pathway for the directional motion of Li^+ ions and at the same time prevent the access of the anions by size exclusion, resulting in good separation of the Li^+ ions and the anions. The conductivity of the reported material is 30 times higher than that of the comparable PEO/Li^+ complex crystal at room temperature. By using state-of-art solid-state NMR spectroscopy, the structure and dynamics of the material were investigated in detail. The dynamics of the Li^+ ions was studied and correlated to the ionic conductivity of the material.*

As a potential solid polymer electrolyte (SPE), polyethylene oxide(PEO)/lithium complex salt (PEO/Li^+) has been intensively investigated for decades.[1–7] Compared to liquid electrolytes, the main shortcoming of SPEs based on PEO/Li^+ complexes lies in the low conductivity over the ordinary temperature range.[8] To improve the conductivity of the PEO/Li^+ complex, research interests firstly focused on the complexed amorphous phase where the random Brownian motion of amorphous polymer segments was considered as the driving force for the Li^+ transportation.[3] Recently, Bruce et al.[9–11] demonstrated that PEO/Li^+ crystalline polymer electrolytes, which were previously thought to be insulators, exhibited marked ionic conductivity, even exceeding their amorphous counterparts. The high ionic conductivity in such materials can be attributed to the directional motion of Li^+ in the nanochannels formed by the PEO chains and the separated anions and cations in the crystal lattice.[12,13] In this scenario, it can be anticipated that increasing the cavity size of the channel while keeping anions and cations well separated probably could further facilitate the Li^+ transportation and thus improve the conductivity.[14] Herein we present a new category of crystalline polymer electrolyte prepared by the supramolecular self-assembly method of Harada[15,16] by using PEO, α-cyclodextrin (α-CD), and $LiAsF_6$. The new type of polymer electrolytes, named as α-CD-PEO/Li^+ complexes, consists of the nanochannels formed by α-CDs in which the PEO/Li^+ complexes are confined. The nanochannels formed by α-CDs provide the pathway for the directional motion of Li^+ ions, and at the same time prevent the access of the anions by size exclusion, resulting in a well separation of Li^+ ions and anions.

The formation of the nanochannels in the α-CD-PEO/Li^+ complex could be probed by ^{13}C cross-polarization/magic angle spinning (CP/MAS) NMR spectroscopy. According to Harada[18] and Li,[19] the formation of the cyclodextrin channel structure can assimilate the conformations of glucose units of CD, leading to the disappearance of the signal splitting in the ^{13}C CP/MAS spectrum.[20] Figure 1a shows the ^{13}C CP/MAS spectra of α-CD, the α-CD-PEO inclusion compound, and the α-CD-PEO/Li^+ complex. The signal splitting in the spectrum of α-CD almost disappears in the spectra of the α-CD-PEO inclusion compound and the α-CD-PEO/Li^+ complex, indicating the formation of cyclodextrin inclusion complex and the nanochannels.[21]

We measured the conductivity of the α-CD-PEO/Li^+ complex. Figure 1b shows the electrochemical impedance spectroscopy (EIS) of the material acquired at 302 K. A semicircle arc connected with a skew line is observed in the spectrum, indicating that the α-CD-PEO/Li^+ complex is a typical electrolyte. In the same figure, the Arrhenius plot of the conductivities is also shown. Fitting the data yields an activation energy of $E_a = 75.1\ kJ\,mol^{-1}$ for the α-CD-PEO/Li^+ complex, which is much lower than that of the PEO/Li^+ crystal ($E_a = 160.4\ kJ\,mol^{-1}$).[17] The low activation energy indicates a low energy barrier for the Li^+ ion motion in the complex sample. This stimulates us to think about the state and dynamics of Li^+ ions in the α-CD-PEO/Li^+ complex sample.

^7Li NMR sprectroscopy, in which different coordination states of Li^+ ions are distinguishable,[22,23] is well suited for studying the state and dynamics of Li^+ ions in the material: The isotropic chemical shift in a MAS NMR spectrum reveals the different coordination states of Li^+ ions; the signal exchange process, which can be recorded by two-dimensional exchange NMR, reflects dynamic coordination-decoordination process of Li^+ ions. Figure 2a shows the ^7Li single pulse spectra of three α-CD-PEO/Li^+ complex samples prepared with different EO:Li^+ feed ratios. It can be seen that the signals in the spectra vary greatly upon varying the EO:Li^+ feed ratios, indicating that the Li^+ ions in these samples may

[*] L.-Y. Yang, D.-X. Wei, M. Xu, Prof. Y.-F. Yao, Prof. Q. Chen
Physics Department & Shanghai Key Laboratory of Magnetic Resonance, East China Normal University
North Zhongshan Road 3663, 200062 Shanghai (P. R. China)
E-mail: yfyao@phy.ecnu.edu.cn
qchen@ecnu.edu.cn

[**] This work was supported by the National Natural Science Foundation of China (20804016, 21174039 and 11005039), Project of Shanghai Committee of Science and Technology (11JC1403600), and the Shanghai Synchrotron Radiation Facility. D.-X.W acknowledges support from the Research Fund for the Doctoral Program of Higher Education.

Supporting information for this article is available on the WWW under http://dx.doi.org/10.1002/anie.201307423.

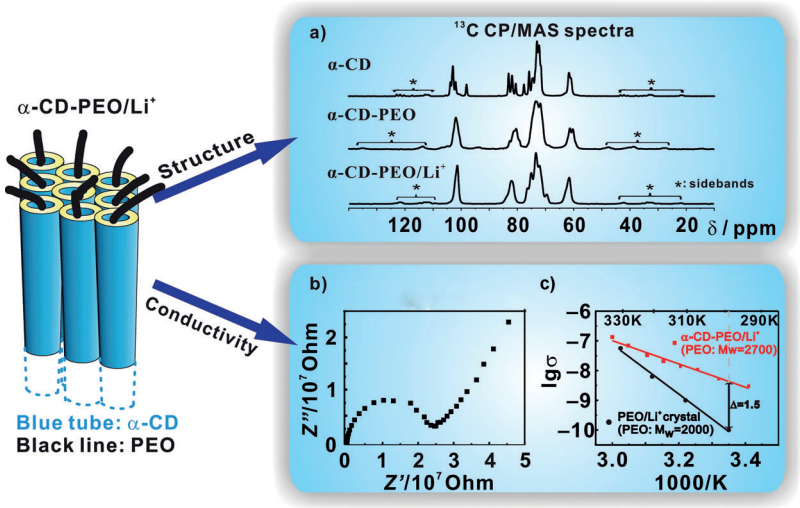

Figure 1. a) ^{13}C CP/MAS spectra of α-CD, α-CD-PEO, and α-CD-PEO/Li$^+$. This α-CD-PEO/Li$^+$ complex was prepared with an ether-oxygen/lithium (EO:Li$^+$) feed ratio of 2:1. b) Electrochemical impedance spectroscopy (EIS) of the same α-CD-PEO/Li$^+$ complex at 302 K and the c) Arrhenius plot of the conductivities. For comparison, the Arrhenius plot of the conductivities of the crystalline polymer electrolyte (PEO_6/$LiSbF_6$, PEO: M_w = 2000)[17] are shown in (c).

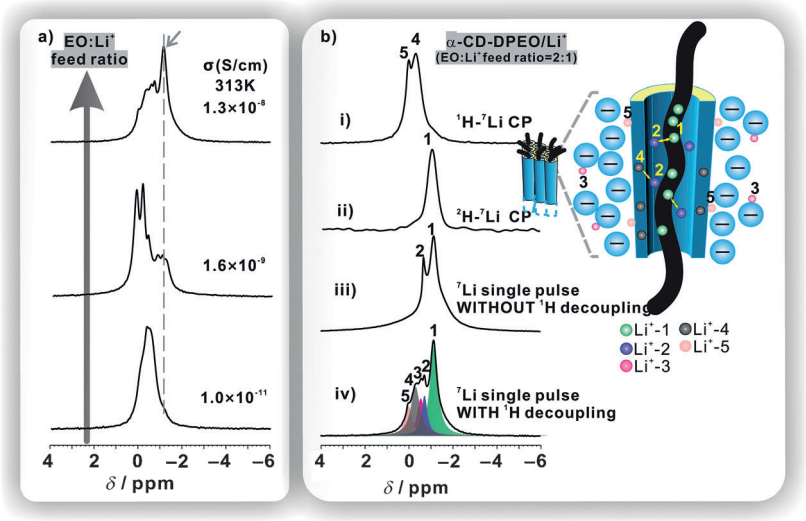

Figure 2. a) ^{7}Li single-pulse excitation spectra of three complexes prepared with different EO:Li$^+$ feed ratios: Top: 2:1, middle: 3:1, bottom: 6:1. ^{1}H decoupling was applied during signal acquisition. b) ^{7}Li spectra of the α-CD-DPEO/Li$^+$ complex (EO:Li$^+$ feed ratio = 2:1): i) ^{1}H–^{7}Li CP/MAS spectrum with ^{1}H decoupling during signal acquisition; ii) ^{2}H–^{7}Li CP/MAS spectrum without ^{1}H decoupling during signal acquisition; iii) ^{7}Li single-pulse excitation spectrum without ^{1}H decoupling during signal acquisition; iv) ^{7}Li single-pulse excitation spectrum with ^{1}H decoupling during signal acquisition. The signal decomposition was carried out by using Dmfit.[27] The illustration shows the exchange processes of the Li$^+$ ions in the nanochannel of the α-CD-DPEO/Li$^+$ complex.

have very different local enviroments. We measured and compared the conductivities of these samples. Interestingly, the conductivities of these samples seem to have a direct correlation to the high field signals (marked by the gray dashed line in the spectra).

To find out the nature of the ^{7}Li signals in the spectra, we prepared an α-CD-PEO/Li$^+$ complex using deuterated PEO (DPEO), named as α-CD-DPEO/Li$^+$. The EO:Li$^+$ feed ratio of this sample is 2:1. Structure characterization shows that this sample has an EO:Li$^+$ ratio of 2.3:1 and an EO:α-CD ratio of 3:1 (see the Supporting Information). By applying the ingenious decoupling and cross-polarization techniques on the deuterated sample,[24–26] we selectively monitored the ^{7}Li$^+$ ions that are located in the proton-enriched environments (close to α-CD) or in the deuteron-enriched environments (close to DPEO) in the sample. Figure 2b shows a series of ^{7}Li NMR spectra of α-CD-DPEO/Li$^+$ acquired in different ways. By using ^{1}H–^{7}Li and ^{2}H–^{7}Li cross-polarization combined with switching on/off ^{1}H decoupling during signal acquisition, the Li$^+$ ions in the ^{1}H enriched environment (close to α-CD) and the ^{2}H enriched environment (close to deuterated PEO) can be selectively monitored. The ^{7}Li NMR spectrum shown in Figure 2b-(i) was acquired through ^{1}H–^{7}Li cross-polarization with ^{1}H decoupling during signal acquisition. In the spectrum, two peaks are clearly resolved (named as Li$^+$-4 and Li$^+$-5). Attributing to the ^{1}H–^{7}Li cross-polarization process, the signals in this spectrum are from the ^{7}Li sites located in the ^{1}H enriched environment. We thus assigned the two signals to the Li$^+$ ions in proximity to the α-CDs. Figure 2b-(ii) shows the ^{7}Li NMR spectrum acquired through ^{2}H–^{7}Li cross-polarization without ^{1}H decoupling during signal acquisition. In the spectrum only one signal (named as Li$^+$-1) is observed and the chemical shift is different from those of the signals in Figure 2b-(i). Similarly, attributing to the ^{2}H–^{7}Li cross-polarization, the signals in this spectrum are likely from the ^{7}Li sites having a ^{2}H enriched environment and thus are assigned to the Li$^+$ ions in proximity to the deuterated PEOs. Figure 2b-(iii) shows the ^{7}Li NMR spectrum acquired using the single pulse excitation without ^{1}H decoupling during signal acquisition. In this spectrum, only the signals from the Li$^+$ ions having no strong ^{1}H–^{7}Li heteronuclear dipolar coupling can be resolved. It is interesting to find that two signals are clearly shown in the spectrum: The upfield signal has a chemical shift exactly equal to the signal in Figure 2b-(ii) and thus assigned to the Li$^+$ ions in proximity to the deuterated PEO. The downfield signal (named as Li$^+$-2) has a chemical shift between the signal Li$^+$-1 and the signal Li$^+$-4. The origin of this signal will be discussed in detail below. Figure 2b-(iv) shows the ^{7}Li NMR spectrum acquired using the single pulse excitation with ^{1}H decoupling during signal acquisition. In this case, the signals from all the ^{7}Li$^+$ ions in the sample can be excited. In the spectrum in Figure 2b-(iv),

multiple peaks are observed. Signal decomposition shows the presence of the signals, Li^+-1, 2, 4, and 5. Additionally, another signal (Li^+-3) is observed between Li^+-2 and Li^+-4. According to the ^7Li spin-lattice relaxation measurement (see the Supporting Information) and ^7Li–^7Li 2D exchange NMR, Li^+-3 is assigned to the "free" Li^+ ions. The signal decomposition shows that the amount ratio of the different Li^+ ion species in the sample Li^+-1:2:3:4:5 is 52:8:10:20:10.

The dynamics of Li^+ ions in the sample was studied by using ^7Li–^7Li 2D exchange NMR. ^1H decoupling during signal acquisition was switched on or off to selectively monitor the Li^+ ions located in the ^1H- or ^2H- enriched environment. Figure 3a shows the ^7Li–^7Li 2D exchange spectrum acquired

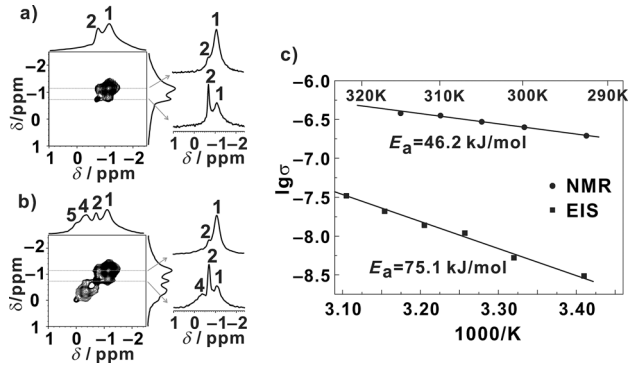

Figure 3. 2D ^7Li–^7Li exchange spectra of the α-CD-DPEO/Li^+ complex acquired by: a) switching off ^1H decoupling during acquisition; b) switching on ^1H decoupling during acquisition. The experimental temperature is 310 K; the exchange time is 300 ms. c) The Arrhenius plot of the conductivities obtained from EIS and from the calculation based on the 2D exchange NMR.

by switching off ^1H decoupling during signal acquisition. In this spectrum, only the Li^+-1,2 signals are resolved, whereas the other ^7Li signals are smeared out by the ^1H–^7Li heteronuclear dipolar coupling. Clear cross-peaks are observed between Li^+-1 and Li^+-2, indicating the presence of the fast exchange process between the Li^+ ions. Figure 3b shows the ^7Li–^7Li 2D exchange spectrum acquired by switching on ^1H decoupling during signal acquisition. In this spectrum, the Li^+-1,2,4,5 signals are resolved. The Li^+-3 signal is missing in Figure 3b because of the short T_1 relaxation time. Interestingly, two sets of cross-peaks, namely the cross-peaks between Li^+-1 and Li^+-2 and the cross-peaks between Li^+-2 and Li^+-4, are observed in the spectrum. This indicates that the Li^+-2 ions likely act as a transmitter, exchanging the Li^+-1 ions (close to the PEO chain) with the Li^+-4 ions (close to the nanochannel; see the illustration in Figure 2b).

To understand the correlation between the macroscopic conductivity and the Li^+ exchange process, we compared the conductivities from EIS and the conductivities estimated from the exchange rates between Li^+-1 and Li^+-2. The variable-temperature ^7Li–^7Li 2D exchange spectra were acquired for this purpose. The exchange rates k (s^{-1}) were estimated by comparing the intensities of the diagonal and cross-peaks. The conductivities were calculated by using Nernst–Einstein equation:[28]

$$\sigma = k\frac{Nq^2l^2}{2k_BT}$$

where N is the concentration of the Li^+ ions, l is the averaged distance between the exchanging Li^+ ions, q is the charge, k_B is the Boltzmann constant, and T is the temperature. More details about the calculation of the conductivity can be found in the Supporting Information. Figure 3c shows the Arrhenius plot of the conductivities from EIS as well as from the calculation based on the 2D exchange NMR. The calculated σ are much higher than those from EIS. This indicates that not all of the Li^+ ion exchange processes contribute to the conductivity of the material. Meanwhile, the activation energy from NMR (46.2 kJ mol^{-1}) is lower than that from EIS (75.1 kJ mol^{-1}), indicating the presence of an additional energetic barrier controlling the macroscopic ionic transport.[29] The grain boundary resistance is considered as one of the important sources that contribute to the additional energetic barrier.

An intriguing feature of the α-CD-PEO/Li^+ complex is that the nanochannel formed by self-assembly of PEO and α-CD provides a pathway for Li^+ transportation, while the cavity size of α-CD prevents the access of the anions $[AsF_6]^-$ by size exclusion. Based on the observations shown above, Figure 2b illustrates the structure and dynamics of the PEO/Li^+ complex in the nanochannel. In such a model, however, several questions still remain unresolved: whether the PEO chain segments "translate" inside the nanochannel, what kind of segmental motion of PEO chain is present in the nanochannel, and whether the segmental motion of PEO chain is coupled with the motion of Li^+ ions. To monitor the dynamics of PEO chains in the nanochannel, temperature-dependent ^2H NMR was performed on the α-CD-DPEO/Li^+ complex.

Figure 4 shows the temperature-dependent ^2H spectra of DPEO, α-CD-DPEO, and α-CD-DPEO/Li^+ complex. The temperature dependent ^2H spectra of DPEO and α-CD-DPEO in Figure 4a and b are very similar to those reported by Beckham[30] and Tonelli.[31] With increasing temperature, the typical Pake lineshape in the spectra of DPEO gradually collapses and, finally becomes a singlet at high temperatures. This characteristic lineshape change can have been attributed to the modulation of a discrete four-site jump present in the *trans–trans–gauche* (*ttg*) conformational sequences of PEO chain[30] (motion model B). In contrast, in the spectra of α-CD-DPEO, the typical Pake lineshape gradually collapses with increasing temperature and finally becomes a typical Pake lineshape with the quadrupolar splitting reduced by a factor of 1/3 at high temperatures. This lineshape change can be attributed to the modulation of a discrete three-site jump present in the *all-trans* conformational sequences of PEO chain[30] (motion model A).

For the α-CD-DPEO/Li^+ complex, the temperature-dependent ^2H spectra (Figure 4c) are similar to the spectra of DPEO (Figure 4a): In the low-temperature range, the typical Pake lineshape with a quadrupolar splitting of 114 kHz is observed in the spectrum; when the temperature

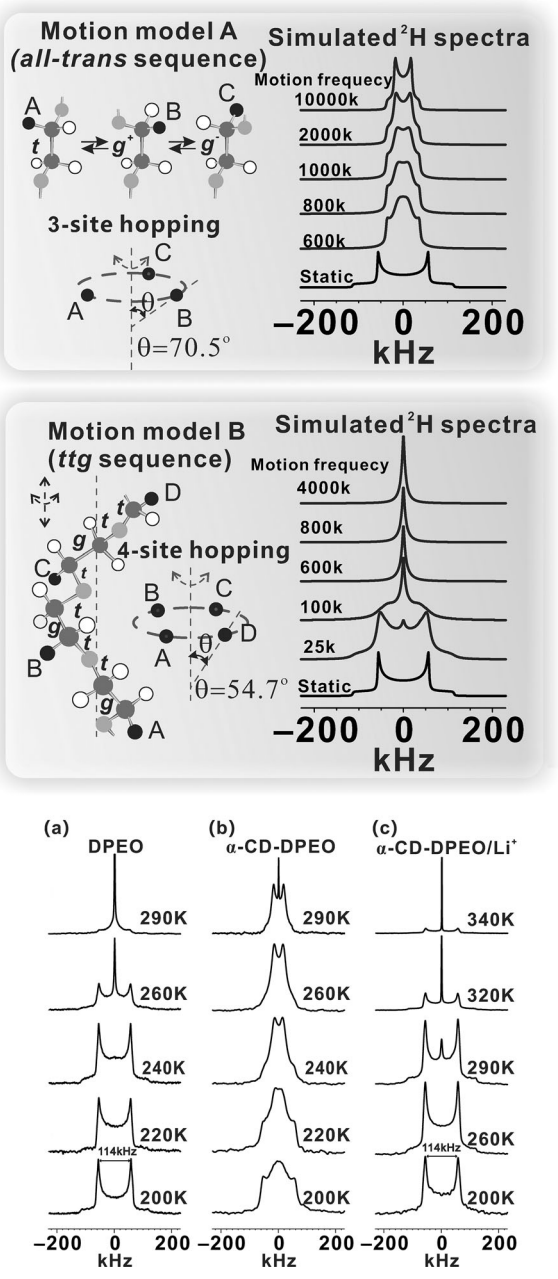

Figure 4. Top: Motion models for the *all-trans* and *trans-trans-gauche (ttg)* sequences of PEO. Bottom: Temperature-dependent ^{2}H spectra of: a) DPEO; b) α-CD-DPEO; and c) α-CD-DPEO/Li^+.

reaches 290 K, a singlet appears in the middle of the Pake pattern. Following Beckham,[30] the appearance of the singlet can be attributed to the modulation of a discrete four-site jump present in the *ttg* conformational sequences of PEO chain (motion model B). This observation (Figure 4c) thus indicates that the PEO chain in the nanochannel of the α-CD-DPEO/Li^+ complex primarily consists of the *ttg* conformational sequences and the discrete four-site jump motion occurs when the temperature reaches 290 K. The structure and dynamics of PEO chain in the nanochannel of the α-CD-DPEO/Li^+ complex thus are completely different from those in the nanochannel of α-CD-DPEO where the *all-trans* conformational sequences and the discrete three-site jump motion are expected. This difference in all likelihood can be attributed to the influence from the coordination between Li^+ ions and PEO chain segments that has been observed in the PEO/Li^+ complex crystals.[32] Note that at 290 K where the discrete four-site jump motion has occurred, the lineshape of the Pake pattern and the distance between the two Pake singularities still remain unchanged. This indicates that while the jump motions occurred, the other parts of the PEO chains in the nanochannel still remain static. In this context, the jump motions in the nanochannels thus can be visualized as the "defects" that move/travel along the nanochannels. Based on these observations, we return to the ^{7}Li–^{7}Li 2D exchange NMR of the α-CD-DPEO/Li^+ complex. The clear exchange process of Li^+ ions (Li^+-1 and Li^+-2) also starts at 290 K (see the Supporting Information). The same starting temperature should thus strongly indicate that the motion of Li^+ ions is coupled to the segmental motion of PEO chain. But at this moment it is still not clear whether it is the jump motion of PEO segments that initiates the Li^+ motion or whether it is the Li^+ motion that initiates the jump motion of PEO segments.

In conclusion, we have presented a new category of crystalline polymer electrolyte by supramolecular self-assembly using PEO, α-cyclodextrin (α-CD), and $LiAsF_6$. This new category of crystalline polymer electrolyte is distinct from the ceramic electrolytes and the PEO/Li^+ crystalline polymer electrolytes. It consists of a nanochannel formed by α-CDs in which the PEO/Li^+ complexes are confined. The nanochannel provides the pathway for the directional motion of Li^+, and at the same time prevents the access of the anions by size exclusion. By combining the ^{7}Li-^{7}Li 2D exchange NMR with the ^{2}H NMR, we have studied the dynamics of Li^+ ions and the PEO segments in the nanochannel in a great detail. These results are considered to have important implications for the design of a new generation of crystalline polymer electrolytes.

Experimental Section

Protonated PEO ($M_w = 2700$) and α-CD were purchased from Sigma–Aldrich, China. Deuterated PEO ($M_n = 2400$) was purchased from Polymer Source, Canada. Lithium hexafluoroarsenate ($LiAsF_6$) was purchased from Alfa Aesar, China.

Preparation of α-CD-PEO/Li^+: A mixture of PEO and $LiAsF_6$ (with a specific EO:Li^+ feed ratio) was dissolved in aqueous solution. This solution then was added to the saturated solution of α-CD. After mixing, the solution became turbid. The turbid solution then was kept for 48 h before centrifugation. The obtained sample was first carefully cleaned using distilled water and then dried in vacuum for a week at 313 K before being used in other experiments.

Solid-state NMR measurements: All of the ^{13}C and ^{7}Li solid-state high-resolution NMR experiments were performed on a Bruker AVANCE III 600 WB spectrometer operating at 150.91, 600.13, and 233.23 MHz for ^{13}C, ^{1}H, and ^{7}Li, respectively. A 4 mm triple resonance MAS probe was used for the expriments. The spin rate was 6 kHz in the ^{1}H–^{13}C CP/MAS experiments and 5 kHz in all the ^{7}Li NMR experiments. The ^{1}H 90° pulse was 4 μs and the spinal64 decoupling sequence was used during signal acquisition. For ^{2}H–^{7}Li cross-polarization, the ^{2}H 90° pulse was 4 μs and the cross-polarization time was 3 ms. For ^{1}H–^{7}Li cross-polarization, the ^{1}H 90° pulse was 4 μs and the cross-polarization time was 500 μs. The 2D ^{7}Li–^{7}Li exchange spectra were recorded under a spinning speed of 5 kHz. The ^{7}Li 90° pulse was 2.3 μs. The mixing times in the experiments were

varied for different exprimental purposes. 32 scans were averaged for each of 2×120 complex t_1 increments. The ^{7}Li and ^{13}C chemical shifts were calibrated using LiCl aqueous solution (1 mol L^{-1}, $\delta = 0$ ppm) and adamantane ($\delta = 38.5$ ppm), respectively.

^{2}H NMR experiments were performed on Bruker AVANCE III 300 WB spectrometer operating at 46.08 MHz by using a homemade static probe. The solid echo pulse sequence was used to record the spectra. The ^{2}H 90° pulse was 2.3 μs. The echo delays were varied between 20 μs to 30 μs.

WXRD and electrochemical impedance spectroscopy (EIS): WXRD measurements were performed on Bruker D8 ADVANCE using Cu Kα (1.5406 Å) radiation (40 kV, 40 mA). All samples were mounted on the same sample holder and scanned from $2\theta = 5°$ to 45° at a speed of 20°/min. The EIS measurements were performed using an electrochemical workstation (AUTOLAB PGSTAT302N). The frequency range is from 100 kHz to 0.01 Hz with the amplitude voltage of 340 mV.

X-ray photoelectron spectroscopy (XPS) experiments were carried out on AXIS Ultra DLD system from Kratos with Al Kα radiation as X-ray source for radiation. The pass energy was 160 eV with the energy step of 1 eV.

Received: August 23, 2013
Revised: November 25, 2013
Published online: March 5, 2014

Keywords: cyclodextrin · inclusion compounds · lithium ions · NMR spectroscopy · polymer electrolytes

[1] D. E. Fenton, J. M. Parker, P. V. Wright, *Polymer* **1973**, *14*, 589.
[2] M. A. Ratner, D. F. Shriver, *Chem. Rev.* **1988**, *88*, 109 – 124.
[3] C. Berthier, W. Gorecki, M. Minier, M. B. Armand, J. M. Chabagno, P. Rigaud, *Solid State Ionics* **1983**, *11*, 91 – 95.
[4] M. Armand, *Adv. Mater.* **1990**, *2*, 278 – 286.
[5] C. Zhang, Y. G. Andreev, P. G. Bruce, *Angew. Chem.* **2007**, *119*, 2906 – 2908; *Angew. Chem. Int. Ed.* **2007**, *46*, 2848 – 2850.
[6] M. Leskes, N. E. Drewett, L. J. Hardwick, P. G. Bruce, G. R. Goward, C. P. Grey, *Angew. Chem.* **2012**, *124*, 8688 – 8691; *Angew. Chem. Int. Ed.* **2012**, *51*, 8560 – 8563.
[7] P. Judeinstein, F. Roussel, *Adv. Mater.* **2005**, *17*, 723 – 727.
[8] C. Tang, K. Hackenberg, Q. Fu, P. M. Ajayan, H. Ardebili, *Nano Lett.* **2012**, *12*, 1152 – 1156.
[9] A. M. Christie, S. J. Lilley, E. Staunton, Y. G. Andreev, P. G. Bruce, *Nature* **2005**, *433*, 50 – 53.
[10] Z. Gadjourova, Y. G. Andreev, D. P. Tunstall, P. G. Bruce, *Nature* **2001**, *412*, 520 – 523.
[11] G. S. MacGlashan, Y. G. Andreev, P. G. Bruce, *Nature* **1999**, *398*, 792 – 794.
[12] C. Zhang, S. Gamble, D. Ainsworth, A. M. Z. Slawin, Y. G. Andreev, P. G. Bruce, *Nat. Mater.* **2009**, *8*, 580 – 584.
[13] S. J. Lilley, Y. G. Andreev, P. G. Bruce, *J. Am. Chem. Soc.* **2006**, *128*, 12036 – 12037.
[14] C. Zhang, E. Staunton, Y. G. Andreev, P. G. Bruce, *J. Am. Chem. Soc.* **2005**, *127*, 18305 – 18308.
[15] A. Harada, J. Li, M. Kamachi, *Nature* **1992**, *356*, 325 – 327.
[16] A. Harada, J. Li, M. Kamachi, *Macromolecules* **1993**, *26*, 5698 – 5703.
[17] Z. Stoeva, I. Martin-Litas, E. Staunton, Y. G. Andreev, P. G. Bruce, *J. Am. Chem. Soc.* **2003**, *125*, 4619 – 4626.
[18] H. Okumura, Y. Kawaguchi, A. Harada, *Macromolecules* **2001**, *34*, 6338 – 6343.
[19] J. Li, X. Ni, Z. Zhou, K. W. Leong, *J. Am. Chem. Soc.* **2003**, *125*, 1788 – 1795.
[20] L. Chen, X. Zhu, D. Yan, Y. Chen, Q. Chen, Y. Yao, *Angew. Chem.* **2006**, *118*, 93 – 96; *Angew. Chem. Int. Ed.* **2006**, *45*, 87 – 90.
[21] J. Xue, Z. Jia, X. Jiang, Y. Wang, L. Chen, L. Zhou, P. He, X. Zhu, D. Yan, *Macromolecules* **2006**, *39*, 8905 – 8907.
[22] H. Wang, H. Kao, T. Wen, *Macromolecules* **2000**, *33*, 6910 – 6912.
[23] Z. Xu, J. F. Stebbins, *Science* **1995**, *270*, 1332 – 1334.
[24] M. Murakami, T. Shimizu, M. Tansho, K. Takegoshi, *Solid State Nucl. Magn. Reson.* **2009**, *36*, 172 – 176.
[25] N. Zumbulyadis, C. J. T. Landry, T. E. Long, *Macromolecules* **1993**, *26*, 2647 – 2648.
[26] N. Zumbulyadis, M. R. Landry, T. P. Russell, *Macromolecules* **1996**, *29*, 2201 – 2204.
[27] D. Massiot, F. Fayon, M. Capron, I. King, S. Le Calvé, B. Alonso, J. O. Durand, B. Bujoli, Z. Gan, G. Hoatson, *Magn. Reson. Chem.* **2002**, *40*, 70 – 76.
[28] a) Á. W. Imre, H. Staesche, S. Voss, M. D. Ingram, K. Funke, H. Mehrer, *J. Phys. Chem. B* **2007**, *111*, 5301 – 5307; b) H. Paul, S. Indris, *J. Phys. Condens. Matter* **2003**, *15*, 1257 – 1289.
[29] a) Ü. Akbey, S. Granados-Focil, E. B. Coughlin, R. Graf, H. W. Spiess, *J. Phys. Chem. B* **2009**, *113*, 9151 – 9160; b) G. R. Goward, M. F. H. Schuster, D. Sebastiani, I. Schnell, H. W. Spiess, *J. Phys. Chem. B* **2002**, *106*, 9322 – 9334.
[30] T. E. Girardeau, J. Leisen, H. W. Beckham, *Macromol. Chem. Phys.* **2005**, *206*, 998 – 1005.
[31] J. Lu, P. A. Mirau, A. E. Tonelli, *Prog. Polym. Sci.* **2002**, *27*, 357 – 401.
[32] Y. Gao, B. Hu, Y. Yao, Q. Chen, *Chem. Eur. J.* **2011**, *17*, 8941 – 8946.

